Reconstruction of the complex angle-dependent photoionization transition dipole from a laser-dressed streaking experiment

Xi Zhao,[1,*] Hui Wei,[1] Wei-Wei Yu,[1,2] and C. D. Lin[1]

[1]*Department of Physics, Kansas State University, Manhattan, Kansas 66506, USA*

[2]*School of Physics and Electronic Technology, Liaoning Normal University, Dalian 116029, People's Republic of China*

(Received 27 June 2018; published 6 November 2018)

We study the retrieval of the angular dependence of the photoionization transition dipole phase of an attosecond XUV pulse in order to reconstruct the whole photoelectron wave packet after the photoemission process. Using a one-electron model Ar atom, we show that the full electron wave packet can be reconstructed from IR-free photoelectron angular distributions and the streaking electron spectra in an IR-dressed XUV photoionization, with photoelectrons along the common polarization direction of the two pulses. The method relies on the validity of the strong-field approximation so it is valid only for higher energy photoelectrons. We also point out that a single photoionization group time delay is not enough to represent a photoemission process; instead, a complete characterization of the electron wave packet requires the retrieval of the spectral phase over the whole bandwidth of the wave packet.

DOI: 10.1103/PhysRevA.98.053404

I. INTRODUCTION

The advent of attosecond technology has opened up the opportunity towards studying the nature of electron dynamics in atomic [1–9], molecular [10–15], and condensed materials [16–19] at the unprecedented time scale [20]. In a typical attosecond streaking experiment, photoelectron spectra are generated by XUV attosecond pulses in the presence of a moderate intense IR laser, with tunable time delay between the two pulses. Traditionally the streaking experiments are used to characterize attosecond pulses in the time domain. If the XUV pulse is an attosecond pulse train (APT), then photoelectrons generated by the XUV can absorb or emit one more photon from the IR field, resulting in sidebands at even harmonic energies. The signals of the sideband will modulate with the time delay at twice the frequency of the IR photon. This method was first used to extract the spectral phase of an APT, and the method is called RABITT (reconstruction of attosecond beating by interference of two-photon transitions) [21,22]. If the XUV is an isolated attosecond pulse (IAP) [23–25], the presence of a streaking IR field would generate a modulating continuum photoelectron spectra as the time delay is varied. Such spectra are called a spectrogram or a spectral trace [26]. It can be used to extract the phase of the IAP using the so-called FROG-CRAB (frequency-resolved optical gating for complete reconstruction of attosecond bursts) method [27]. Since the spectral intensity of the APT and the IAP can be extracted directly from the IR-free single-photon XUV ionization of atoms, combining the retrieved spectral phase of the XUV pulse allows the reconstruction of the attosecond pulse in the time domain. In both applications, the IR field should be moderate such that IR alone does not ionize the atom. The method also requires accurate knowledge of the target atom which can be obtained from synchrotron radiation experiment or from theoretical calculation. In most of the streaking experiments, both the linearly polarized XUV and IR pulses have the same polarization direction, which is to be called the z axis, and photoelectrons are measured only along the z axis.

To retrieve the phase of an IAP, an accurate and simple theory for IR-dressed photoelectron spectra is required. The strong-field approximation (SFA) [28] is a simple theory, but it is not accurate for describing the streaking spectra when the photoelectron energy is less than, say, 30 or 40 eV. Still it is the only theory available today for retrieving the spectral phase. In fact, additional assumptions are used in the FROG-CRAB method, thus results retrieved using the FROG-CRAB method have to be taken with caution [29,30]. In particular, the so-called central momentum approximation was used in FROG-CRAB. This approximation is not valid for broadband pulses. Algorithms have been developed such as the PROBP (phase retrieval of broadband pulses) [31] and the VTGPA (Volkov-transform generalized projection algorithm) [32]. Both methods can be used to retrieve the spectral phase of broadband pulses.

It is obvious that if the phase of the XUV pulse is known, then the same spectrogram may be used to retrieve the atomic properties. Since an IR-free XUV photoionization experiment allows the determination of the amplitude of the one-photon transition dipole, ideally the goal is to obtain the phase of the transition dipole from the spectrogram. Having both transition dipole amplitude and phase for single-photon ionization along the polarization axis, one retrieves the full photoelectron wave packet along the z axis. On the other hand, photoionization also generates electrons at other angles. In principle one would like to determine the whole electron wave packet over all the angles [33,34]. Using APTs, such questions have been addressed in a recent experiment by Heuser *et al.* [35]. We are not aware of similar experiments performed with IAPs so far.

*zhaoxi719@phys.ksu.edu

This article is organized as the following: Sec. II introduces the theoretical background and the relevant mathematical expressions, including the derivation of the angular-dependent transition dipole and the SFA model of the streaking measurement. Section III discusses our two-step method for phase retrieval in detail. Several examples are given in Sec. IV to demonstrate the performance of our method in which the input spectrograms are simulated by the SFA model and by solving the time-dependent Schrödinger equation (TDSE), respectively. We conclude this work in Sec. VI by emphasizing that it is preferable to retrieve the amplitude and phase of the atomic dipole, in particular, in terms of the partial wave decomposition, instead of the oversimplification of the prevailing "photoionization time delays" studies for electrons emerging along the polarization axis only. Atomic units are used throughout this article unless mentioned.

II. ANGULAR DEPENDENCE OF THE AMPLITUDE AND PHASE OF PHOTOELECTRON WAVE PACKET

In this article, we are interested in retrieving the whole electron wave packet when a one-electron atom is photoionized by an isolated attosecond pulse. For clarity, we first derive the expression of the photoelectron wave packet following the elementary quantum theory for a one-electron atom and the spin is not included. The atomic Hamiltonian is given as

$$H_0 = -\frac{\nabla^2}{2} + V(r). \tag{1}$$

Specifically we treat a one-electron model argon atom. The electron is under the influence of a model potential $V(r)$ which is parametrized as in Tong and Lin [36] in the form of

$$V(r) = \frac{-Z_c + a_1 e^{-a_2 r} + a_3 r e^{-a_4 r} + a_5 e^{-a_6 r}}{r}. \tag{2}$$

Here $Z_c = 1$ is the asymptotic charge seen by the electron. The potential in Eq. (2) can also be expressed as the sum of the Coulomb potential $-1/r$ and a remaining short-range potential. We can solve the time-independent Schrödinger equation numerically to obtain the bound and continuum wave functions. The initial state,

$$\langle \mathbf{r}|\, i\rangle = R_{n_i l_i}(r) Y_{l_i m_i}(\hat{r}), \tag{3}$$

has well-defined orbital angular momentum l_i, m_i is the magnetic quantum number, $R_{nl}(r)$ is the radial wave function, and Y_{lm} is the spherical harmonic. The continuum state in which the emitted photoelectron has energy $E = \frac{k^2}{2}$ and direction $\hat{k}$ can be constructed by partial wave expansion as

$$|E\hat{k}\rangle = \sum_{LM} e^{-i\eta_L(E)} Y^*_{LM}(\hat{k}) |ELM\rangle, \tag{4}$$

$$\langle \mathbf{r}|\, ELM\rangle = R_{EL}(r) Y_{LM}(\hat{r}), \tag{5}$$

where $R_{EL}(r)$ is the energy-normalized radial wave function of the continuum state, $\eta_L(E) = -\frac{L\pi}{2} + \sigma_L(E) + \delta_L(E)$ is the phase shift for the partial wave with angular quantum number L, $\sigma_L = \arg[\Gamma(L+1-iZ_c/k)]$ is the Coulomb phase shift, and δ_L is the phase shift due to the short-range potential. In spherical coordinates the direction of the electron momentum $\hat{k}$ can be denoted by the polar angle θ_k and azimuthal angle φ_k.

Consider one-photon ionization by an XUV pulse. Choose the z axis as the polarization axis of the light. In the frequency domain the XUV pulse is expressed by $\tilde{E}_{\mathrm{XUV}}(\Omega)$. Then we can write down the wave packet of the photoelectron based on the first-order time-dependent perturbation theory as

$$\begin{aligned}|\psi(t)\rangle &= \sum_{lm} \int dE\, \tilde{E}_{\mathrm{XUV}}(E+I_p) e^{-iEt} \langle Elm|z|n_i l_i m_i\rangle |Elm\rangle \\ &= \int dE\, \tilde{E}_{\mathrm{XUV}}(E+I_p) e^{-iEt} \big\{ \big\langle R_{E,l_i-1}\big|r\big|R_{n_i,l_i}\big\rangle \\ &\quad \times \big\langle Y_{l_i-1,m_i}\big|\cos\theta_r\big|Y_{l_i,m_i}\big\rangle \big|E(l_i-1)m_i\big\rangle \\ &\quad + \big\langle R_{E,l_i+1}\big|r\big|R_{n_i,l_i}\big\rangle \big\langle Y_{l_i+1,m_i}\big|\cos\theta_r\big|Y_{l_i,m_i}\big\rangle \\ &\quad \times |E(l_i+1)m_i\rangle \big\}. \end{aligned} \tag{6}$$

Here I_p is the ionization potential of the initial bound state. In photoelectron measurements, usually one projects this wave packet onto a stationary state $|E\hat{k}\rangle$, that is,

$$\langle E\hat{k}|\psi(t)\rangle = \tilde{E}_{\mathrm{XUV}}(E+I_p) d(E,\hat{k}) e^{-iEt}. \tag{7}$$

The modulus square of Eq. (7) gives the photoelectron yield measured in the direction $\hat{k}$. Removing the electric field of the XUV from Eq. (7), we obtain the complex angular-dependent dipole matrix element:

$$\begin{aligned} d(E,\hat{k}) &= e^{i\eta_{l_i-1}(E)} Y_{l_i-1,m_i}(\hat{k}) \big\langle R_{E,l_i-1}\big|r\big|R_{n_i,l_i}\big\rangle \\ &\quad \times \big\langle Y_{l_i-1,m_i}\big|\cos\theta_r\big|Y_{l_i,m_i}\big\rangle + e^{i\eta_{l_i+1}(E)} Y_{l_i+1,m_i}(\hat{k}) \\ &\quad \times \big\langle R_{E,l_i+1}\big|r\big|R_{n_i,l_i}\big\rangle \big\langle Y_{l_i+1,m_i}\big|\cos\theta_r\big|Y_{l_i,m_i}\big\rangle. \end{aligned} \tag{8}$$

While the modulus square of Eq. (8) can be deduced from single-photon ionization measurement, its phase is not available. If the phase can be measured, then we can say that the full electron wave packet from the simple photoionization experiment by the known attosecond pulse is completely determined.

To simplify the analysis, take the Ar atom as an example where $n_i = 3$, $l_i = 1$. Denote the radial matrix elements as $W_L(E) = \langle R_{EL}|r|R_{31}\rangle$. By working out the angular part we have

$$\begin{aligned} d_0(E,\hat{k}) &= \sqrt{\frac{1}{12\pi}} \{ W_0(E) e^{i\eta_0(E)} \\ &\quad + W_2(E) e^{i\eta_2(E)} (3\cos^2\theta_k - 1) \}, \end{aligned} \tag{9}$$

for the case where the initial state has $m_i = 0$. For the initial state with $m_i = \pm 1$, we have

$$d_{\pm 1}(E,\hat{k}) = \pm \sqrt{\frac{3}{8\pi}} W_2(E) e^{i\eta_2(E)} \cos\theta_k \sin\theta_k e^{\pm i\varphi_k}. \tag{10}$$

In most of the previous so-called photoionization time delay experiments and theories the amplitude and phase of the photoelectron wave packet is studied along $\theta_k = 0^\circ$ only. In fact, what have been reported usually is not the phase of the dipole, but rather the first derivative of the phase with respect to the energy of the electron. Such a derivative in optics in general is called group delay, but it has been widely called "photoemission time delay" in the attosecond science

community [37,38]. If there is only one partial wave (as is the case for $m_i = \pm 1$) contributing to the phase, this group delay is similar to the Wigner time delay [39,40] which was defined for the phase of a fixed angular momentum quantum number. We will use Wigner time delay to mean the first derivative of the dipole phase with respect to electron energy. Since the dipole phase in Eq. (8) is dependent on the scattering angle of the photoelectron, one can ask the angle-dependent dipole phase or the angle-dependent Wigner time delay. For photoelectrons along the polarization axis, the phase or the Wigner time delay have been extracted from analyzing XUV+IR streaking spectra. To obtain the same quantities at other angles, does one need to examine streaking photoelectron spectra along each direction of the photoelectron? The angular dependence of photoelectron time delay has been investigated recently in experiments and in simulations [7,34] if the XUV is an APT. To our knowledge, no similar studies have been carried out using isolated attosecond pulses yet. Can one extend the streaking method to obtain the phases of photoelectrons emerging at other angles?

In standard photoionization experiment, the measured angular resolved single-photon ionization electron spectra is the average of the three ionization channels since the experiment in general does not select the initial values of m_i. Thus the photoionization differential cross section is given by

$$\frac{d\sigma}{d\Omega_k} \propto \frac{1}{3}\{|d_0(E,\hat{k})|^2 + |d_{+1}(E,\hat{k})|^2 + |d_{-1}(E,\hat{k})|^2\}. \tag{11}$$

One can easily calculate from Eqs. (9) and (10),

$$\frac{d\sigma}{d\Omega_k} = \frac{\sigma_{\text{total}}(E)}{4\pi}[1 + \beta(E)P_2(\cos\theta_k)], \tag{12}$$

where $\sigma_{\text{total}}(E)$ is the total cross section. In this work,

$$\sigma_{\text{total}}(E) = \frac{1}{3\pi}|W_0(E)|^2 + \frac{2}{3\pi}|W_2(E)|^2, \tag{13}$$

and the β parameter,

$$\beta(E) = \frac{2|W_2(E)|^2 + 4W_0(E)W_2(E)\cos[\eta_0(E) - \eta_2(E)]}{|W_0(E)|^2 + 2|W_2(E)|^2}. \tag{14}$$

From these expressions, at each energy E, the measured $\sigma_{\text{total}}(E)$ and $\beta(E)$ from XUV photoionization alone would not allow the determination of the four parameters needed to characterize the complex dipole matrix elements in Eqs. (9) and (10). Thus additional measurements would be needed. Like streaking experiments for electrons along the z axis, would the angular distributions of photoelectrons from the nonlinear IR-dressed XUV ionization allow us to obtain the other parameters needed such that the whole electron wave packet along any directions can be obtained?

The amplitude and phase of Eq. (9) are shown in Fig. 1 for the case of $m_i = 0$. Both exhibit strong angular dependence. For the case of $m_i = \pm 1$, according to Eq. (10), there is no angular dependence in the dipole phase. This would correspond to the simplest case where the wavefront of the electron wave packet does not depend on the scattering angles. To isolate such a simple case, the electron has to be ionized from a specific initial $m_i = \pm 1$. The results in Fig. 1 are obtained from solving the time-independent Schrödinger

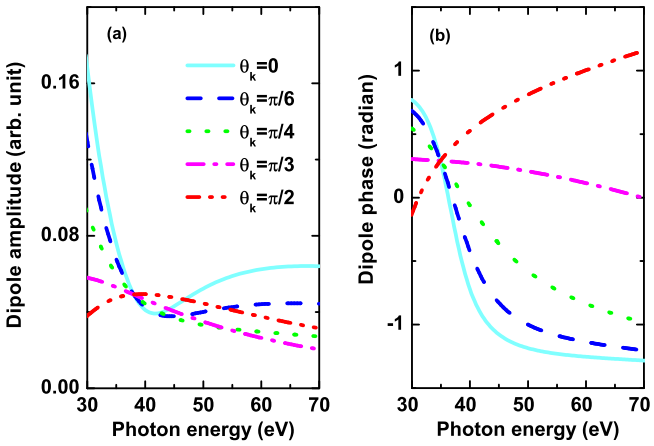

FIG. 1. Angular dependence of single-photon dipole transition amplitude (a) and phase (b), $d_0(E,\theta_k)$, for the case of ionization from the $m_i = 0$ initial $3p$ state of Ar. They are calculated from Eq. (9) where the radial matrix element and phase for the two partial waves $L = 0$ and 2 are obtained from solving the time-independent Schödinger equation.

equation. They are the angular-dependent dipole amplitude and phase for photoelectrons emitted after ionization by an XUV pulse. In this article we ask what experiments should be done in order to obtain the results shown in Fig. 1.

In streaking experiments, the photoionization process happens in a dressing IR field. Because of the IR field, the electron spectra will be modified compared to the laser-free case. Assume both the XUV and IR are polarized along the z axis, and the peak of the XUV pulse is delayed by τ with respect to the IR peak field. We can model the angular-dependent streaking spectrogram by SFA:

$$S(\mathbf{p},\tau) = \frac{1}{3}\sum_{m=-1,0,1}\left|\int_{-\infty}^{\infty} E_{\text{XUV}}(t-\tau)d_m[\mathbf{k}(t)] \times e^{-i\int_t^{\infty}(pA(t')\cos\theta + \frac{1}{2}A^2(t'))dt'} e^{i(\frac{p^2}{2}+I_p)t}dt\right|^2. \tag{15}$$

In Eq. (15), $\mathbf{A}(t) = \hat{z}A(t) = -\hat{z}\int_{-\infty}^{t} E_{\text{IR}}(t')dt'$ is the vector potential of the IR field. The measured photoelectron momentum vector is $\mathbf{p}$. In spherical coordinates it can be expressed by (p,θ,φ), and the measured electron energy $E_p = \frac{p^2}{2}$. Equation (15) includes the transition dipoles $d_m[\mathbf{k}] = d_m(E = k^2/2, \hat{k})$ which are given by Eqs. (9) and (10). However, in the situation of XUV+IR streaking, $\mathbf{k}$ is a time-dependent variable,

$$\mathbf{k}(t) = \mathbf{p} + \mathbf{A}(t). \tag{16}$$

Using spherical coordinates, $\varphi_k = \varphi$, and

$$k(t) = \sqrt{p^2 + A^2(t) + 2pA(t)\cos\theta}, \tag{17}$$

$$\theta_k(t) = \arctan\frac{p\sin\theta}{p\cos\theta + A(t)}. \tag{18}$$

Due to the streaking effect, the photoelectron observed at an angle θ involves single-photon ionization toward a range

of angles θ_k, as demonstrated by Eq. (18). In addition, the streaking experiment is most likely carried out without the selection of m_i of the $3p$ electron, thus the dipole phase of the different initial m_i also occurs in Eq. (15) for each streaking spectra in a given direction. To extract the dipole phase at a given direction away from the polarization axis, the whole angular streaking spectra over the whole angular range of the photoelectron and the spectral range of the XUV pulse have to be analyzed at the same time. To retrieve so many parameters at the same time clearly looks impossible. Simplification occurs only for $\theta = 0^\circ$, then $\theta_k = 0^\circ$ or 180°. In that special case, only the $m_i = 0$ channel contributes to the electron spectrum. For $\theta = 0^\circ$, for example,

$$S(\mathbf{p},\tau) = \left| \int_{-\infty}^{\infty} E_{\mathrm{XUV}}(t-\tau) d_0[k(t)] \times e^{-i\int_t^{\infty}(pA(t')+\frac{1}{2}A^2(t'))dt'} e^{i(\frac{p^2}{2}+I_p)t} dt \right|^2. \quad (19)$$

III. METHOD OF RETRIEVING ANGULAR ATOMIC DIPOLE PHASE

The goal of this work is to retrieve the angle-resolved transition dipole. In view of the complications just discussed, an alternative method is proposed here. According to Eq. (9) once we have obtained W_0, W_2, η_0, and η_2, the dipole amplitude in any direction can be calculated. One possible approach is to retrieve these four functions over the spectral bandwidth of the XUV pulse from the IR-dressed streaking spectra over the whole angular range. This is still too complicated as well since there are too many parameters to be retrieved. Instead, here we propose a two-step retrieving process. First, from the IR-free photoelectron angular distributions we have $\sigma_{\mathrm{total}}(E)$ and $\beta(E)$ within the bandwidth of the XUV pulse. From Eqs. (13) and (14) we can derive

$$3\pi\sigma_{\mathrm{total}}(E)[1-\beta(E)] = |W_0(E)|^2 - 4W_0(E)W_2(E)\cos[\eta_0(E)-\eta_2(E)]. \quad (20)$$

The left-hand side of Eq. (20) is a known function, whereas the four unknown functions on the right-hand side can be combined into two, $W_0(E)$ and $G(E) = W_2(E)\cos[\eta_0(E) - \eta_2(E)]$. We expand the two unknowns by B-spline functions:

$$W_0(E) = \sum_i a_i B_i^k(E), \quad (21)$$

$$G(E) = \sum_j b_j B_j^k(E). \quad (22)$$

The unknown coefficients $\{a_i, b_j\}$ are optimized by genetic algorithm (GA) in order to obtain the best fit to the left-hand side of Eq. (20). From the retrieved $W_0(E)$, one can calculate $W_2(E)$ from Eq. (13). Then from the retrieved $G(E)$ one can deduce the phase shift difference $\eta_0(E) - \eta_2(E)$.

Figures 2(a) and 2(b) are the input σ_{total} and β parameter for Ar atoms. Mathematically, Eq. (20) is a simple quadratic function of the unknowns, therefore it only takes a few seconds for our GA solver to converge. After about 18 000 generations we obtained $W_0(E)$ and $G(E)$, then from Eq. (14), we also obtain the phase difference $\eta_0 - \eta_2$. Figures 2(c) and 2(d) compare

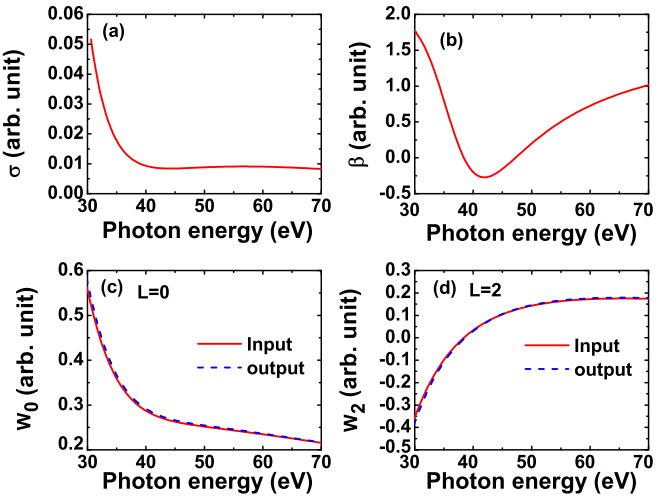

FIG. 2. Retrieval of the radial matrix elements from IR-free photoelectron angular distributions. (a) Input total cross section σ_{total}. (b) Input β parameter. (c) Input and retrieved radial matrix element W_0. (d) The same but for W_2. The phase difference between the two partial waves vs photon energy from the input and from the retrieval also agree well (not shown).

the input and retrieved radial matrix elements W_0 and W_2. The input and retrieved data match very well. The retrieved phase difference $\eta_0 - \eta_2$ also agrees well with the input data. Thus if we can retrieve one of the phases within the spectral range, we would have retrieved all the parameters. We can obtain this unknown from the spectrogram for photoelectrons along the polarization axis, which would give the phase of the atomic transition dipole along that direction. Once this phase is retrieved, using the known W_0, W_2, and $\eta_0 - \eta_2$, from Eq. (9), all the four parameters W_0, W_2, η_0, and η_2 as functions of E are obtained. In retrieving the atomic dipole phase, we employed the PROBP method [30,31] which is superior to FROG-CRAB since the latter employs central momentum approximation.

IV. RESULTS

A. Test with high energy spectrogram generated from SFA

Since the XUV is weak, the IR-free photoelectron angular distributions can be calculated exactly by first-order perturbation theory. In the IR-dressed XUV photoionization, we first assume that the photoelectron spectrogram along the polarization direction can be calculated using the SFA equation. The SFA approximation works reasonably well for XUV photon energy at and above about 60 eV. Here we choose three different XUV pulses. One is a transform-limited (TL) pulse and the other two are chirped pulses. They share the same spectral amplitude which takes a Gaussian form with a central photon energy of 60 eV and a full width at half maximum (FWHM) bandwidth of 11.5 eV. The TL pulse has a FWHM duration of 160 as and a peak intensity of 10^{12} W/cm^2. The FWHM duration of the two chirped pulses are 280 as and 400 as, respectively. The IR field is 800 nm in wavelength, cosine-squared envelope, 4.4 fs in FWHM duration, 10^{12} W/cm^2 in peak intensity, and the carrier-envelope phase (CEP) is zero.

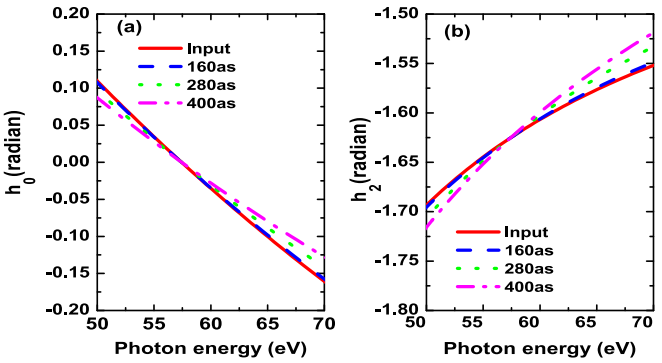

FIG. 3. Test of the accuracy of the retrieved partial wave phase shift (a) η_0 and (b) η_2. The streaking spectra are generated using the SFA with the known input parameters. Three XUV pulses that have the same spectral amplitude but different spectral phases are used to generate the Ar spectrograms. The two phases retrieved from the three spectrograms are compared to the input phases. Larger-chirp pulses give larger errors, but the error is very small, about 0.01 radians or less. Parameters used (see text). The center energy of the XUV pulse is at 60 eV.

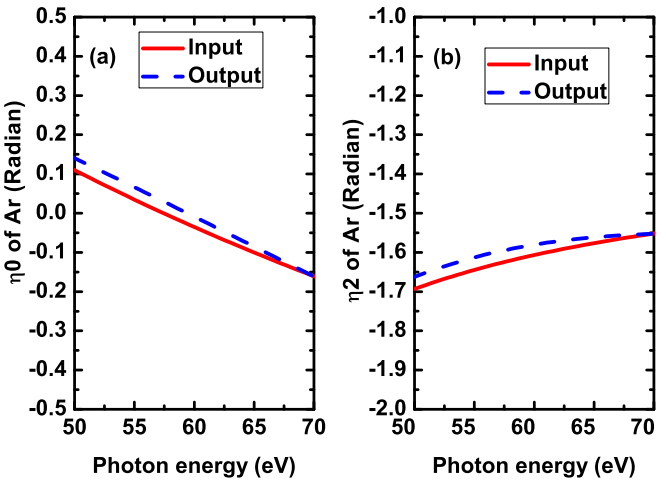

FIG. 4. The same as Fig. 3 but the spectrogram was generated from the solution of the TDSE. Only un-chirped TL pulse is used. Larger error of about 0.04 radians or less can be seen but the error is quite acceptable.

The three XUV pulses should give the same IR-free photoelectron angular distributions since in first-order theory, the spectral phase of the XUV does not affect the cross sections. In the presence of an IR field, the spectrograms for the three IR-dressed XUV pulses are different; the retrieved phase shifts η_0 and η_2 can be different. Figure 3 shows the comparison of the retrieved phase shifts with the input ones. For the TL input pulse, the two phase shifts η_0 and η_2 can be accurately extracted, as they lie on top of the input results. For the 280-as chirped pulse, the error in the retrieved phase shifts is about 0.01 radians or less and for the 400-as chirped pulse, the error is about 0.025 radians or less. Such errors originate from the iterative retrieval processes. Such small errors in the input and output results are tolerable. If one accounts for the errors in the signal, the errors seen here will be easily surpassed. Based on these results, we conclude that the input results can be retrieved accurately with the methods and algorithms presented here.

We should mention here, in the first retrieval step we obtain $W_0(E)$ and $G(E)$ from the parameter fitting. In the calculation of W_2 from W_0 using Eq. (13) we need to take the square root, thus, there are actually two branches of solutions—one with positive sign and the other with negative sign. Both branches should be considered in the second step. We did two separate optimizations in the retrieval of η_0; each corresponds to one choice of W_2. The solution that can best fit the input IR-dressed spectrogram is chosen to be our final retrieved result.

B. Test with high energy spectrogram generated from TDSE

Next we use the spectrogram simulated by solving the TDSE as the input data. Since the retrieval is based on the SFA model, larger errors than the previous simulations are expected. Here we use the same TL XUV pulse as in Fig. 3 (with a central photon energy of 60 eV) to generate the TDSE data. The retrieved η_0 and η_2 are plotted in Fig. 4 to compare with the input ones. Even using the TDSE data as the input, the error of phase shift retrieval is quite small (within 0.05 radians). This shows that both η_0 and η_2 can be accurately retrieved when using XUV pulses with central photon energy of about 60 eV for the Ar target investigated here if the streaking spectra were taken from the experiment which should be closer to the TDSE spectra.

C. Test with low-energy spectrogram generated from TDSE

In yet another example, we use a TL XUV pulse whose bandwidth is the same as before but its central photon energy is reduced to 40 eV. From this new input IR-dressed spectrogram that is simulated by TDSE, we repeat our method to retrieve η_0 and η_2. The results are plotted in Fig. 5. In this example, the error in the retrieved phase is about 0.25 to 0.5 radians. This is not surprising since it has been well established that the SFA model does not accurately describe low-energy photoelectrons (16–34 eV in this example). Thus one has to conclude that it is not possible to accurately retrieve the partial wave phase shifts, or equivalently, the phase of low energy photoelectrons. This means that the electron wave packet generated by the XUV one-photon ionization cannot be accurately reconstructed.

D. Photoionization dipole phase or photoionization time delay?

Using the retrieved W_0, W_2, η_0, and η_2, we can calculate the angle-dependent transition dipole phases using Eqs. (9) and (10). Since the dipole phase in Eq. (10) for $m_i = \pm 1$ is independent of θ_k, we only show in Fig. 6 the input and retrieved dipole phase for $m_i = 0$ on the plane of the emission angle θ_k and the photon energy within the bandwidth of the XUV pulse. The center of the photon energy is 40 eV, thus this example is for low-energy photoelectrons.

The phase plots in Fig. 6, together with the photoelectron angular distribution would give the maximal information in an XUV photoionization experiment. Such information would allow us to reconstruct the time-dependent electron wave

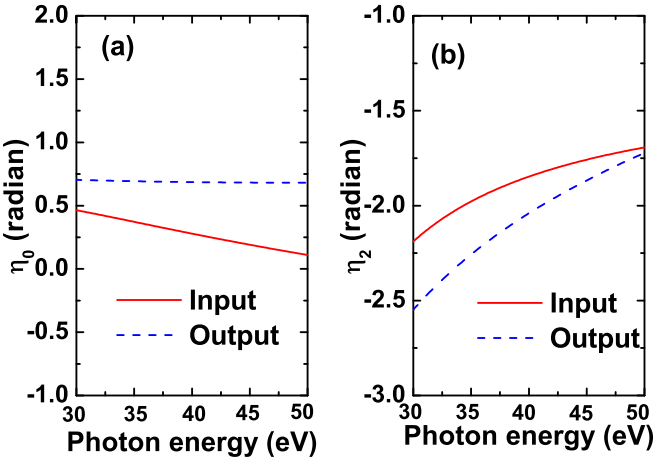

FIG. 5. Retrieval of partial wave phase shift (a) η_0 and (b) η_2 from a TDSE-simulated Ar spectrogram using a transform-limited XUV pulse. The central photon energy in this example is 40 eV. Much larger errors of about 0.5 radians or less in the retrieved phase shifts can be seen. This example shows that accurate phase shifts cannot be retrieved for low-energy photoelectrons. The failure is due to the strong field approximation used in the phase retrieval algorithm which is not valid for low-energy electrons.

packet generated by the XUV pulse (see below). Consider Fig. 6(a); the dipole phase calculated using Eq. (9) with W_0, W_2, η_0, and η_2 obtained from solving the time-independent Schrödinger equation clearly differs from Fig. 6(b) where the dipole phase is obtained using the retrieved radial matrix elements and partial wave phase shifts (see Fig. 5). On the other hand, one can see some resemblance between Figs. 6(a) and 6(b). It means that the error in SFA declines gradually as the photoelectron energy is increased, as demonstrated by better agreement of the two graphs at higher photon energy. The same set of data can also be compared in terms of Wigner group delay [see Fig. 7(a) vs Fig. 7(b)] by taking the derivative of the phase in Fig. 6(b) at each angle with respect to energy. Again, the two figures in Figs. 7(a) and 7(b) do not agree, but a certain similarity can be observed. The dark blue regions in Figs. 7(a) and 7(b) are due to the Cooper minimum in the photoionization cross section of Ar $3p$. Cooper minimum occurs when the cross section goes through a minimum in a small energy range. In quantum physics, it amounts to the phase of the electron wave undergoing a rapid change of close to π in this narrow energy region, or equivalently the derivative of the phase with respect to energy is large (in absolute value). Thus Cooper minimum occurs in the energy and angular region where the group delay is large. Figures 7(a) and 7(b) show that the group delay is large only for emission angles less than about 40°, which is consistent with the minima in the angular distributions shown in Fig. 1(a). For larger angles, there is no large group delay and there is no Cooper minimum in the photoelectron spectra.

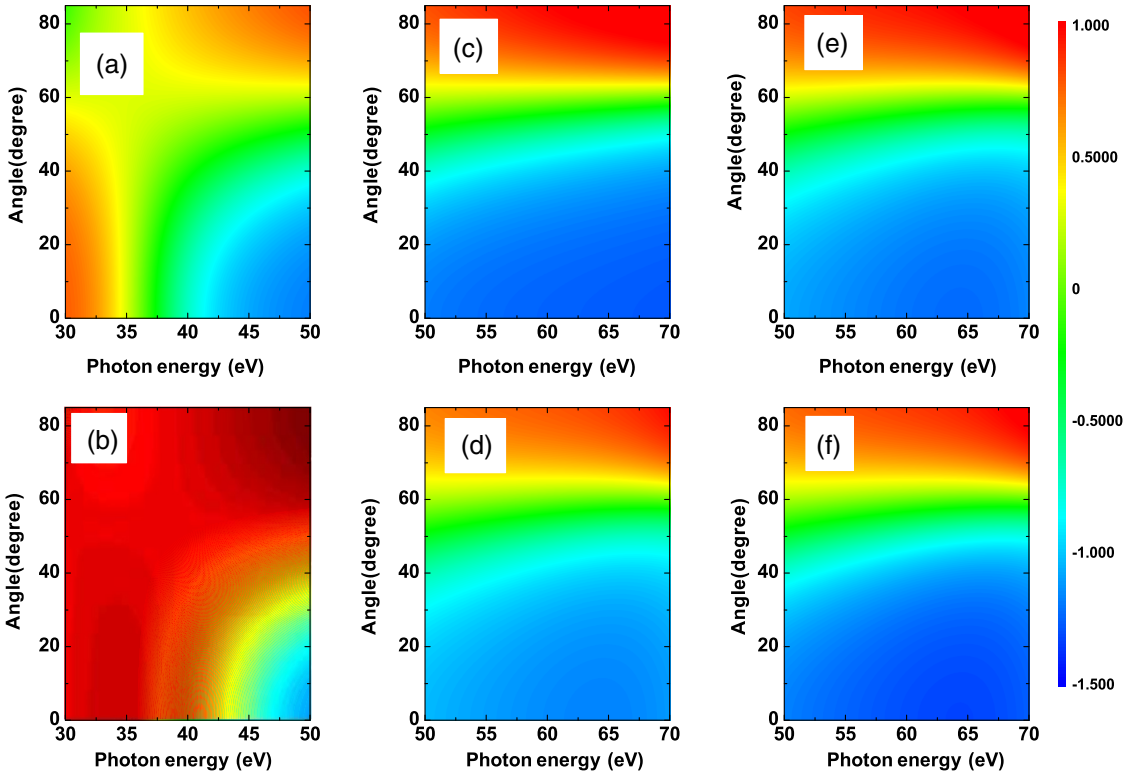

FIG. 6. Comparison of the retrieved and the input transition dipole phase arg$[d_0(E, \theta_k)]$ (unit, radian) for $m_i = 0$ as functions of both the photon energy $E + I_p$ and the emission angle θ_k. The central photon energy is 40 eV in (a) and (b) and 60 eV in (c)–(f). (a) and (c) The input data; (b) and (d) the reconstructed dipole phase by the retrieved W_0, W_2, η_0, and η_2, where η_0 and η_2 are obtained from TDSE-simulated spectrograms using transform-limited XUV pulses with the duration of 160 as (see Figs. 4 and 5). (e) and (f) The reconstructed dipole phase where η_0 and η_2 are obtained from SFA-simulated spectrograms using two chirped XUV pulses with the duration of (e) 280 as and (f) 400 as, respectively; also see Fig. 3. Accurate retrieval of the phase over the whole range of electron energies and angles can be seen except in (b).

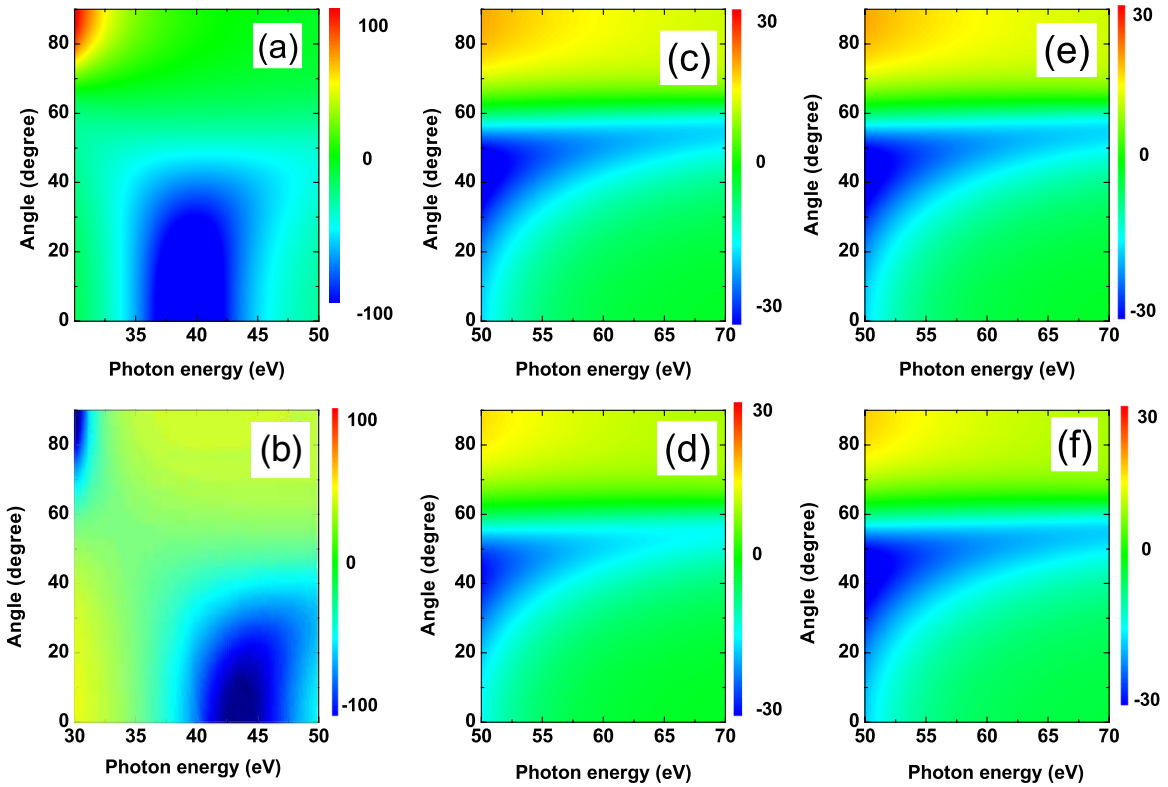

FIG. 7. Comparison of the retrieved and the input Wigner group delay $\tau^W(E,\theta_k) = \frac{d}{dE}\arg[d_0(E,\theta_k)]$ (unit, as) for $m_i = 0$. These graphs are identical to those in Fig. 6 except that the Wigner delays are shown here.

In Figs. 6(c)–6(f), we compare the dipole phase results for central photon energy at 60 eV. The input dipole phases in two dimensions are shown in Fig. 6(c). In Fig. 6(d), the retrieved dipole phases are obtained from streaking spectra calculated from solving the TDSE and the XUV is transform-limited (160 as). As expected, the agreement with the input data is excellent. For the retrieved dipole phases shown in Figs. 6(e) and 6(f), the streaking spectra were generated using the SFA model with chirped XUV pulses of 280 as and 400 as, respectively. For both chirped pulses, the dipole phases [Figs. 6(e) and 6(f)] or the group delays [Figs. 7(e) and 7(f)] retrieved using the methods used here are in good agreement with the input. Thus we can conclude that the XUV photoionization dipole phase can be retrieved accurately if the central photon energy is about 60 eV and higher.

V. EXTRACTING TRANSITION DIPOLE PHASE OR PHOTOIONIZATION TIME DELAY FROM THE STREAKING SPECTRA?

The results from Fig. 6 show that the full photoelectron wave packet generated by an XUV single attosecond pulse at all the angles can be accurately retrieved with the help of an IR pulse if photon energy is near 60 eV and above. With the amplitude and phase accurately retrieved over the whole bandwidth and momentum directions, the time dependence of the whole electron wave packet in the coordinate space can be reconstructed from

$$\left|\Psi_{m_i,\hat{k}}(\mathbf{r},t)\right\rangle = \int dE\,\tilde{E}_{\mathrm{XUV}}(E+I_p)e^{-iEt}d_{m_i}(E,\hat{k})|E\hat{k}\rangle. \tag{23}$$

Note that the stationary continuum state with the given electron energy E and propagation direction $\hat{k}$ is given by the wave function $|E\hat{k}\rangle$, Eq. 4, which is the eigenstate of the field-free Hamiltonian. This is the electron wave packet associated with ionization from the $3p$ shell with a particular magnetic quantum number. For the photoelectron ionized from each initial state, $3p_0$, $3p_{-1}$, or $3p_{+1}$, each has its own coherent wave packet, and each wave packet has its own angular dependence. There is no meaning to add these three wave packets directly since they are associated with different degenerate ionic cores, corresponding to different channels. If the magnetic quantum number is not determined experimentally, then the total streaking spectra is given by an expression like Eq. (15). The dipole phase (or the Wigner delay) cannot be directly retrieved from the streaking spectra except along the z direction where only the $3p_0$ channel is ionized.

Since Wigner delay is the derivative of the phase with respect to the electron energy, if one extracts the Wigner delay at each energy point within the spectral bandwidth, then the use of the dipole phase or Wigner delay are equivalent as one can be obtained from other, up to an unimportant constant phase. However, from the analysis in Sec. II, it shows that there is no advantage of replacing the phase by the group delay. For example, in the model Ar atom used here, the

electron wave packets are written naturally in terms of phases and amplitudes. The wave packet in coordinate space, as given in Eq. (23), is also expressed in terms of phases. In this regard, it is important to note that an averaged group delay for the three wave packets associated with the three m_i's would have no meaning since the Wigner group delay is defined only with respect to the wave packet, not with respect to the electron density.

While it may be tempting to generalize the present wave-packet retrieval to a many-electron system, it is hard to see how realistic this can be done. In the description of photoionization processes in the energy domain for a many-electron system, each channel is no longer described by a partial wave phase shift, but rather by a complex scattering amplitude of the S matrix. In the energy domain, each complex amplitude is given by $d_{m_i,j}(E,\hat{k})$ where j is the index for the channel. It would be a monumental task to extract these complex scattering amplitudes from experimental spectra since it would take multiparameter coincidence measurements to separate channels.

Most of the present-day experiments with single attosecond pulses either measure IR-dressed photoelectron spectra like the streaking spectra discussed here or with attosecond transient absorption spectroscopy (ATAS). In the former, the majority of experiments have reported photoionization time delays for atoms, molecules, solids, and liquids (see reviews [38]). In these experiments, usually a single group delay difference between two species or between two channels of the same species at the center of the XUV photon energy was reported. To obtain this single group delay difference, the center of mass of the electron spectra is evaluated at each XUV-IR delay τ. By comparing the time delay τ_j where the center of mass of the streaking spectra for channel j peaks, a single photoionization time delay difference $\tau_{12} = \tau_1$-τ_2 was obtained from the experimental spectra directly. This simple procedure eliminates the tedious phase retrieval steps like the one we presented here.

The procedure described above for extracting the delay difference from the measured streaking spectra is quite straightforward, but what is the meaning of this photoionization delay difference? In the best-case scenario this difference is the group delay difference of the two electron wave packets associated with the two channels. However, a group delay of a wave packet at a given photon energy point gives no information about the wave packet. This amounts to specifying the group delay at a single point in one of the two-dimensional frames of Fig. 7(a) along the line where the angle $\theta_k = 0$. More seriously, information is carried by the whole wave packet, not by a part or one energy point of the wave packet. In this article we stress that the whole electron wave packet emerging from the photoionization of our model atom is represented by Eq. (23). As this wave packet propagates in "time," its wave front evolves in the radial as well as the angular dimensions. "Time" in this picture is a parameter, not a measured quantity.

Before closing this section, we want to point out that electron streaking spectra ejected at different angles have been reported in experiments using APT+IR pulses [35] using the RABITT method. Since in APT spectra the energy gap between two neighboring energy points is twice the IR photon energy and the phase entering the sidebands is the phase of the two-photon transition matrix element, it does not give the transition dipole phase by the XUV pulse directly.

VI. DISCUSSION AND CONCLUSIONS

In this article we proposed a method to obtain the angular-dependent transition dipole phase in the elementary single photoionization of an atom by an isolated attosecond XUV pulse. While the dipole phase has been studied using the streaking spectra generated by IR-dressed XUV photoionization spectrogram, the method has been limited to the electron wave packet along the direction of the polarization axis only. To obtain dipole phases for the whole electron wave packet, a two-step method was proposed. It relies on retrieving the partial wave radial dipole matrix elements and the associated scattering phases. Based on elementary quantum theory, we showed that these parameters can be fully retrieved from the IR-free photoionization angular distributions, together with the IR-dressed photoelectron streaking spectra along the polarization axis. Taking a model Ar atom as an example, we also showed that the dipole phase can be obtained accurately only when the XUV photon energy is about 60 eV and above. Since the phase retrieval method employs the strong field approximation which is invalid for low-energy photoelectron streaking, the spectral phases for low-energy electrons cannot be retrieved.

ACKNOWLEDGMENTS

This research was supported in part by Chemical Sciences, Geosciences and Biosciences Division, Office of Basic Energy Sciences, Office of Science, U.S. Department of Energy, under Grant No. DE-FG02-86ER13491. W.-W.Y. would also like to acknowledge the partial support of the Chinese Scholarship Council (CSC), and the National Natural Science Foundation of China under Grant No. 11604131.

[1] M. Drescher *et al.*, Nature (London) **419**, 803 (2002).
[2] P. Eckle, A. N. Pfeiffer, C. Cirelli, A. Staudte, R. Dörner, H. G. Muller, M. Büttiker, and U. Keller, Science **322**, 1525 (2008).
[3] M. Schultze *et al.*, Science **238**, 1658 (2010).
[4] M. Swoboda, T. Fordell, K. Klünder, J. M. Dahlström, M. Miranda, C. Buth, K. J. Schafer, J. Mauritsson, A. L'Huillier, and M. Gisselbrecht, Phys. Rev. Lett. **104**, 103003 (2010).
[5] K. Klunder, J. M. Dahlstrom, M. Gisselbrecht, T. Fordell, M. Swoboda, D. Guenot, P. Johnsson, J. Caillat, J. Mauritsson, A. Maquet, R. Taieb, and A. L'Huillier, Phys. Rev. Lett. **106**, 143002 (2011).
[6] C. Ott *et al.*, Nature (London) **516**, 374 (2014).
[7] C. Palatchi, J. M. Dahlström, A. S. Kheifets, I. A. Ivanov, D. M. Canaday, P. Agostini, and L. F. Di Mauro, J. Phys. B: At., Mol. Opt. Phys. **47**, 245003 (2014).

[8] M. Sabbar, S. Heuser, R. Boge, M. Lucchini, T. Carette, E. Lindroth, L. Gallmann, C. Cirelli, and U. Keller, Phys. Rev. Lett. **115**, 133001 (2015).
[9] V. Gruson *et al.*, Science **354**, 734 (2016).
[10] G. Sansone *et al.*, Nature (London) **465**, 763 (2010).
[11] H. J. Wörner, J. B. Bertrand, D. V. Kartashov, and P. B. Corkum, and D. M. Villeneuve, Nature (London) **466**, 604 (2010).
[12] J. Caillat, A. Maquet, S. Haessler, B. Fabre, T. Ruchon, P. Salières, Y. Mairesse, and R. Taïeb, Phys. Rev. Lett. **106**, 093002 (2011).
[13] F. Kelkensberg, W. Siu, J. F. Perez-Torres, F. Morales, G. Gademann, A. Rouzee, P. Johnsson, M. Lucchini, F. Calegari, J. L. Sanz-Vicario, F. Martin, and M. J. J. Vrakking, Phys. Rev. Lett. **107**, 043002 (2011).
[14] F. Calegari *et al.*, Science **346**, 336 (2014).
[15] A. Trabattoni, M. Klinker, J. Gonzalez-Vazquez, C. Liu, G. Sansone, R. Linguerri, M. Hochlaf, J. Klei, M. J. J. Vrakking, F. Martin, M. Nisoli, and F. Calegari, Phys. Rev. X **5**, 041053 (2015).
[16] A. L. Cavalieri *et al.*, Nature (London) **449**, 1029 (2007).
[17] S. Neppl *et al.*, Nature (London) **517**, 342 (2015).
[18] R. Locher *et al.*, Optica **2**, 405 (2015).
[19] Z. Tao, C. Chen, T. Szilvási, M. Keller, M. Mavrikakis, H. Kapteyn, and M. Murnane, Science **353**, 62 (2016).
[20] C. D. Lin, A. T. Le, C. Jin, and H. Wei, *Attosecond and Strong-Field Physics Principles and Applications* (Cambridge University Press, Cambridge, 2018).
[21] P. M. Paul, E. S. Toma, P. Breger, G. Mullot, F. Augé, P. Balcou, and H. G. Muller, and P. Agostini, Science **292**, 1689 (2001).
[22] E. S. Toma and H. G. Muller, J. Phys. B **35**, 3435 (2002).
[23] M. Hentschel *et al.*, Nature (London) **414**, 509 (2001).
[24] E. Goulielmakis *et al.*, Science **320**, 1614 (2008).
[25] K. Zhao, Q. Zhang, M. Chini, Y. Wu, X. Wang, and Z. Chang, Opt. Lett. **37**, 3891 (2012).
[26] J. Itatani, F. Quéré, G. L. Yudin, M. Y. Ivanov, F. Krausz, and P. B. Corkum, Phys. Rev. Lett. **88**, 173903 (2002).
[27] Y. Mairesse and F. Quéré, Phys. Rev. A **71**, 011401 (2005).
[28] M. Kitzler, N. Milosevic, A. Scrinzi, F. Krausz, and T. Brabec, Phys. Rev. Lett. **88**, 173904 (2002).
[29] H. Wei, T. Morishita, and C. D. Lin, Phys. Rev. A **93**, 053412 (2016).
[30] X. Zhao, H. Wei, C. Wei, and C. D. Lin, J. Opt. **19**, 114009 (2017).
[31] X. Zhao, Hui Wei, Yan Wu, and C. D. Lin, Phys. Rev. A **95**, 043407 (2017).
[32] P. D. Keathley, S. Bhardwaj, J. Moses, G. Laurent, and F. X. Kärtner, New J. Phys. **18**, 073009 (2016).
[33] J. Wätzel, A. S. Moskalenko, Y. Pavlyukh, and J. Berakdar, J. Phys. B: At. Mol. Opt. Phys. **48**, 025602 (2015).
[34] A. Mandal, P. C. Deshmukh, A. S. Kheifets, V. K. Dolmatov, and S. T. Manson, Phys. Rev. A **96**, 053407 (2017).
[35] S. Heuser, A. JimenezGalan, C. Cirelli, C. Marante, M. Sabbar, R. Boge, M. Lucchini, L. Gallmann, I. Ivanov, A. S. Kheifets, J. M. Dahlstrom, E. Lindroth, L. Argenti, F. Martin, and U. Keller, Phys. Rev. A **94**, 063409 (2016).
[36] X. M. Tong and C. D. Lin, J. Phys. B: At., Mol. Opt. Phys. **38**, 2593 (2005).
[37] A. Maquet, J. Caillat and R. Taïeb, J. Phys. B: At., Mol. Opt. Phys. **47**, 204004 (2014).
[38] R. Pazourek, S. Nagele, and J. Burgdörfer, Rev. Mod. Phys. **87**, 765 (2015).
[39] E. P. Wigner, Phys. Rev. **98**, 145 (1955).
[40] F. T. Smith, Phys. Rev. **118**, 349 (1960).